First-principles molecular dynamics studies of liquid selenium close to the critical point

1999 J. Phys.: Condens. Matter 11 10211

(http://iopscience.iop.org/0953-8984/11/50/313)

J. Phys.: Condens. Matter **11** (1999) 10211–10218. Printed in the UK PII: S0953-8984(99)08394-0

First-principles molecular dynamics studies of liquid selenium close to the critical point

R Stadler†, G Kresse‡ and M J Gillan†

† Physics and Astronomy Department, University College London, Gower Street, London WC1 6BT, UK

‡ Institute for Theoretical Physics of the Technical University of Vienna, Wiedner Hauptstrasse 8-10/136, A-1040 Vienna, Austria

Received 4 October 1999

Abstract. First-principles molecular dynamics simulations of liquid selenium for three different densities at the temperatures 1770 and 1870 K are presented. Whereas the densities for 1770 K have been chosen to correspond to pressures at which recent x-ray diffraction experiments were performed, the densities for 1870 K are related to pressures close to the critical point in the p–T phase diagram. For the lower temperature, close agreement with the most recent x-ray data is found in structure factors and pair distribution functions. For the higher temperature, the structure factors get large at low wavelengths close to the critical point. This indicates a highly compressible liquid as would be expected within the critical regime.

1. Introduction

Unlike in other elemental liquids, the atoms in liquid selenium (l-Se) are twofold coordinated in a chainlike structure as deduced from diffraction experiments [1]. This chain structure arises from covalent bonding and is closely related to the existence of a band gap and a low electrical conductivity at temperatures below the critical point ($T_c = 1860$ K, $p_c = 380$ bar) [2]. The pressure–temperature phase diagram with contours of dc conductivity is shown in figure 1.

The static structure factor of l-Se up to 1673 K was measured by means of neutron diffraction in the pioneering work of Edeling and Freyland [1]. In recent x-ray diffraction experiments, Tamura and co-workers [3–5] investigated the static structure of l-Se up to temperatures only ∼100 K below the critical point, covering a wide region of semiconducting and also metallic phases of the liquid. The thermodynamic states at which their measurements were performed are indicated with open circles in figure 1.

l-Se was first studied by means of first-principles molecular dynamics (FPMD) simulations by Hohl and Jones [6]. They employed the local density approximation (LDA) within the formalism of density functional theory (DFT) and found a branched network of chains with rather short chain lengths, where the average twofold coordination of Se atoms only prevails by onefold- and threefold-coordinated atomic positions balancing each other. A similar picture was obtained by Bichara and co-workers [7, 8] using a tight-binding Monte Carlo approach. However, studying l-Se at temperatures of 570, 870 and 1370 K along the liquid–vapour coexistence curve, Kirchhoff *et al* [9,10] were able to show that within DFT the agreement with experimental static structure factors could be substantially improved by using the generalized gradient approximation (GGA) in the parametrization of Perdew and Wang [11]. In their calculations, the fraction of twofold-coordinated atoms is almost 100% near the melting point.

0953-8984/99/5010211+08$30.00

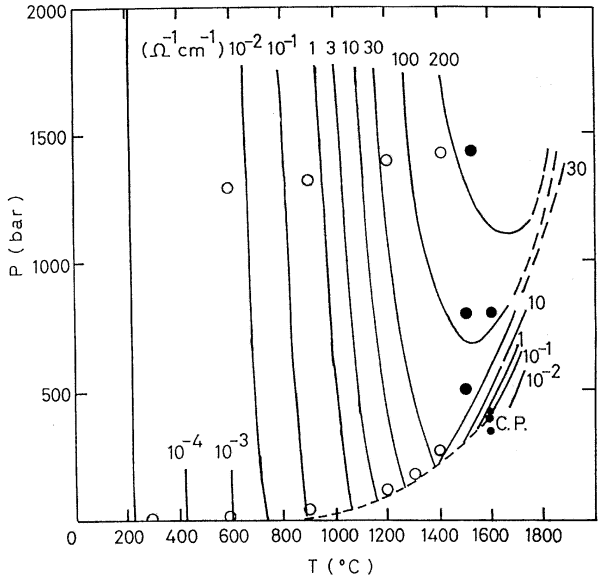

Figure 1. A pressure–temperature phase diagram with contours of constant dc conductivity for l-Se [2, 12]. Open circles indicate thermodynamic states for which x-ray diffraction experiments were performed [3–5]; full circles indicate the states for our calculations.

The geometry and electronic structure of the defects were also examined in depth by the same authors [12]. Very recently, Shimojo *et al* [13] performed FPMD calculations within a DFT–GGA framework, following the higher line of open circles—indicating states where diffraction experiments were carried out—in figure 1 up to metallic states of l-Se.

The aim of the present work is to investigate the static structure of l-Se for a range of densities/pressures at high temperatures, especially close to the critical point and even slightly below the liquid–vapour coexistence curve. The thermodynamic states that we investigated are marked by full circles in figure 1. The first vertical line of points at 1770 K coincides with states for which diffraction measurements have been presented in references [3–5], whereas to the best of our knowledge no experimental or theoretical investigation of l-Se at 1870 K has been undertaken so far.

2. Simulation methods

We performed our FPMD simulations within a DFT–GGA framework using the pseudopotential approximation and plane-wave basis sets. All of our calculations were carried out by employing the well-established first-principles simulation code VASP [14–16]. The details of the pseudopotential and GGA parameters are the same as in references [9–12]. Our periodically repeated box contained 69 atoms. Using the Nosé–Hoover thermostat technique [17], the equations of motion were solved with a time step of 3 fs for all systems studied. A total simulation time of 4.5 ps was separated into 1.5 ps for equilibration and 3 ps for sampling of properties. In our (N, V, E) calculations the pressure and temperature were allowed to fluctuate. While the time average of the temperature was fixed to the values marked in figure 1 by our thermostat technique, for simulating the corresponding pressures we made use of experimental density isobars [5] and pressure isochores [18]. With the help of these data

we related a pressure in figure 1 to the experimentally found density at a given temperature and kept this density constant during our simulations. Temperatures, densities, number densities and pressures for all of the states that we have studied are given in table 1.

Table 1. The temperatures T, densities ρ and number densities n at which simulations were done. Also shown are the experimental pressures p_{exp}, the calculated numbers of nearest neighbours N_c and the self-diffusion coefficients D, where the values in parentheses show D calculated from the VACF; for details see the text.

T (K)	ρ (g cm^{-3})	n (Å^{-3})	p_{exp} (bar)	N_c	D (10^{-9} m^2 s^{-1})
1770 K	3.25	0.0248	1420	1.91	27.1 (27.6)
	3.13	0.0239	815	1.80	28.5 (30.8)
	2.94	0.0224	515	1.82	28.4 (29.7)
1870 K	3.09	0.0235	815	1.85	30.5 (31.2)
	2.68	0.0204	420	1.80	23.9 (22.8)
	2.20	0.0169	370	1.76	34.5 (37.0)

3. Results and discussion

In figures 2 and 3 the static structure factor $S(k)$ and the pair distribution function $g(r)$ at 1770 K are compared with experimental data from references [3, 4] and [19] measured at 1773 K. The static structure factor provides the most direct means of comparison with diffraction data and is derived from

$$S(k) = \langle |\hat{\rho}_{\boldsymbol{k}}|^2 \rangle \tag{1}$$

in our calculations. Here, the dynamical variable $\hat{\rho}_{\boldsymbol{k}}$ represents the density of atoms at wavevector $\boldsymbol{k}$:

$$\hat{\rho}_{\boldsymbol{k}} = N^{-1/2} \sum_{i=1}^{N} \exp(\mathrm{i}\boldsymbol{k} \cdot \boldsymbol{R}_i) \tag{2}$$

where the sum goes over all N atoms in the system. From figure 2 it can be seen that the agreement of $S(k)$ taken from our calculations (solid lines) with the values from references [3–5] (dashed lines) is reasonable but far from being perfect. In particular, at 1420 bar (figure 2(a)) the first maximum and minimum of the experimental curve are shifted towards larger $\boldsymbol{k}$-vectors compared to our calculations. Additionally, a distinct kink occurs at about 3 Å^{-1} that is not found in our MD runs. Going to lower densities (figures 2(b) and 2(c)) the same shift is found, but less pronounced. A slight kink in the experimental curve at 815 bar (figure 2(b)) can still be seen, but at 515 bar (figure 2(c)) no such feature is visible. On the other hand, the experimental data from reference [19] at 815 bar (the dotted line of figure 2(b)) agree with our simulation to a very high degree. No kink can be found in this curve and, at least up from the first minimum, $S(k)$ becomes identical to the function derived from our calculations where also for lower wavevectors the agreement improves substantially compared with the dashed curve. Looking at the pair distribution functions $g(r)$ in figure 3 a similar behaviour can be observed. Again at 815 bar (figure 3(b)) the agreement between our calculated function (the solid line) and that from reference [19] is excellent, although the calculated first maximum is slightly higher and the second maximum slightly lower than in the diffraction experiment. Also in references [10] and [13] it was found that in all of the cases studied the height of the second maximum predicted by GGA–DFT calculations was distinctly lower than in experimental measurements. Comparing to the diffraction data

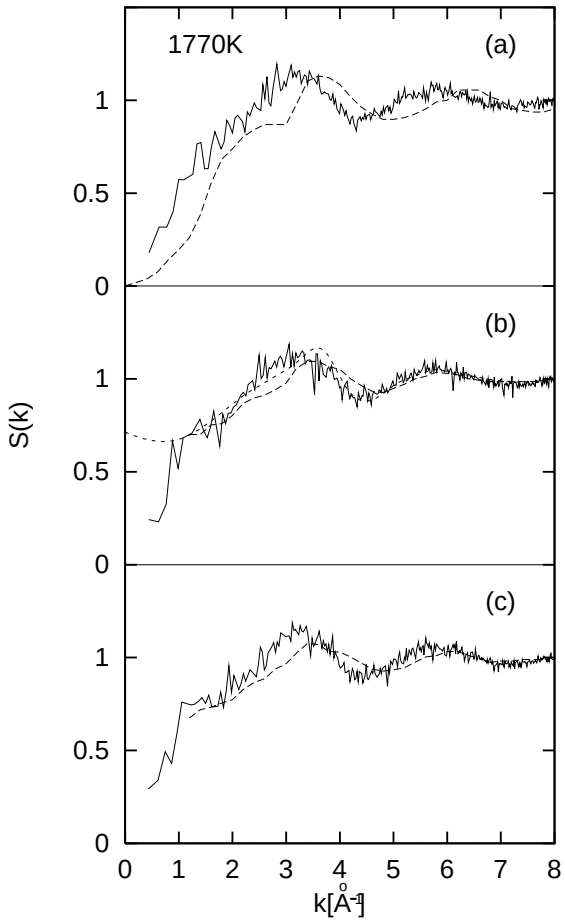

Figure 2. Static structure factors $S(k)$ for calculations at 1770 K and (a) 1420 bar, (b) 815 bar, (c) 515 bar. Solid lines denote values from our calculations; dashed and dotted lines refer to x-ray experiments from references [3–5] and reference [18], respectively.

from references [3–5] (dashed lines), again much less agreement can be found, especially at the highest pressure, 1420 bar (figure 3(a)). In this case even the position of the first maximum (corresponding to the average bonding length for covalent bonds) is shifted to a value of 2.28 Å in the function taken from experiment. Tamura [4] suggested a model which explains this bond shortening as due to the occurrence of short-chain molecules with a planar zigzag conformation where π-bonds between next-nearest neighbours increase the bonding strength, therefore decreasing the bonding distance. We could not find evidence for such planar molecules from any configuration of our MD run at 1770 K and 1420 bar. Soldo *et al* [20] performed EXAFS experiments for liquid selenium at various temperatures and found a shift towards similarly low next-neighbour distances at 1670 and 1770 K. However, since these measurements were performed at 600 bar, they cannot confirm diffraction data at 1420 bar. Alternatively, the EXAFS results should be compared with the available diffraction results at 515 (figure 3(a)) and 815 bar (figure 3(b)) from reference [3] where no shift of the first peak towards smaller radii can be found. At 1420 bar all of the experimental peak heights differ from our calculations in figure 3(a). Going to lower pressures the agreement improves, and for

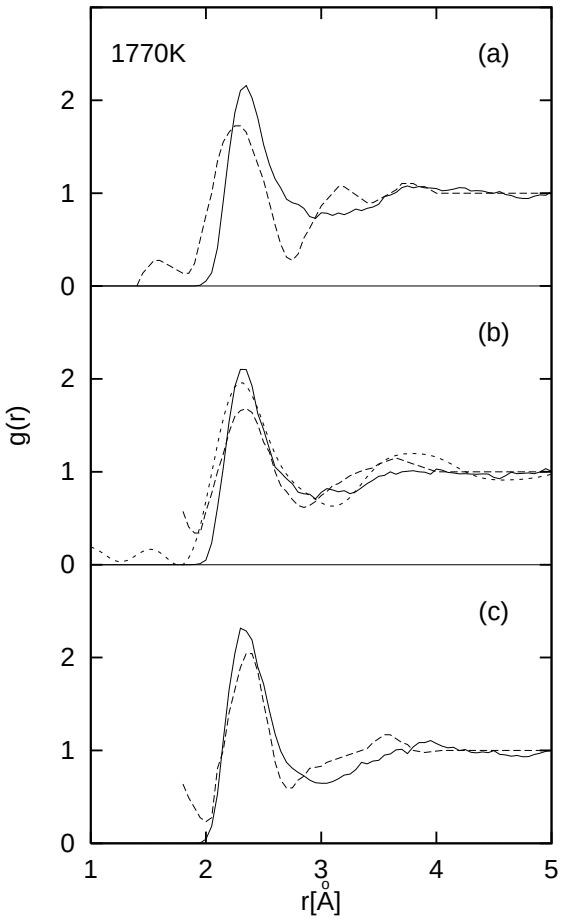

Figure 3. Pair distribution functions $g(r)$ for calculations at 1770 K. The pressures for (a)–(c) and the key to the different line types are as for figure 2.

515 bar (figure 3(c)) it becomes acceptable. Although both diffraction data sets refer to work from the same group, the data from references [3,4] were obtained from weak 'in-house' x-ray sources and have large uncertainties whereas the measurements in reference [19] have been performed using synchrotron radiation and provide much more reliable results [21]. Therefore, we conclude that our description of the static properties of l-Se at 1770 K is reasonably accurate since the level of agreement with the so far most reliable diffraction experiments is very high. Unfortunately, no experimental data obtained using a synchrotron have become available for the states at 515 and 1420 bar so far.

In the last two columns of table 1 the average coordination number N_c and the self-diffusion constant D for all systems studied are listed. N_c has been derived by integrating $g(r)$ up to a fixed temperature-independent value of 2.85 Å; D has been derived using the Einstein relation

$$2tD = \frac{1}{3}\langle|\boldsymbol{r}_i(t) - \boldsymbol{r}_i(0)|^2\rangle \tag{3}$$

in the long-time limit $t \to \infty$ and, alternatively, by studying the time integral of the velocity autocorrelation function (VACF) as described in reference [9] (values in parentheses). The values for N_c at 515 and 815 bar are lower than that for the higher pressure as would be

expected, since the volume per atom is higher in these cases. All values are lower than 2, reflecting low chain lengths at high temperatures as was found in reference [10]. The pressure dependence of the diffusion coefficient is very low; the results for 515 and 815 bar are nearly identical, and at 1420 bar the mobility of the atoms is slightly reduced.

In figures 4 and 5 the functions $S(k)$ and $g(r)$, respectively, are given for our calculations at 1870 K. No experimental data are available at a temperature so close to the critical point at 1860 K. The lower two of the three depicted pressures, 370 and 420 bar, are slightly above and slightly below the critical pressure of 380 bar which is also illustrated in figure 1. The highest pressure, however, was chosen to be 815 bar for the sake of comparison with our calculations at 1770 K. Most strikingly, in figures 4(a) and 4(b), $S(k)$ reaches high values at small wavevectors. This is exactly what would be expected near the critical point since the isothermal compressibility κ_T is related to the static structure factor by

$$\lim_{k\to 0} S(k) = nk_BT\kappa_T \tag{4}$$

where n is the number density and k_B is Boltzmann's constant. A large value of $S(k \to 0)$ therefore indicates a highly compressible liquid or in other words critical behaviour. Similar

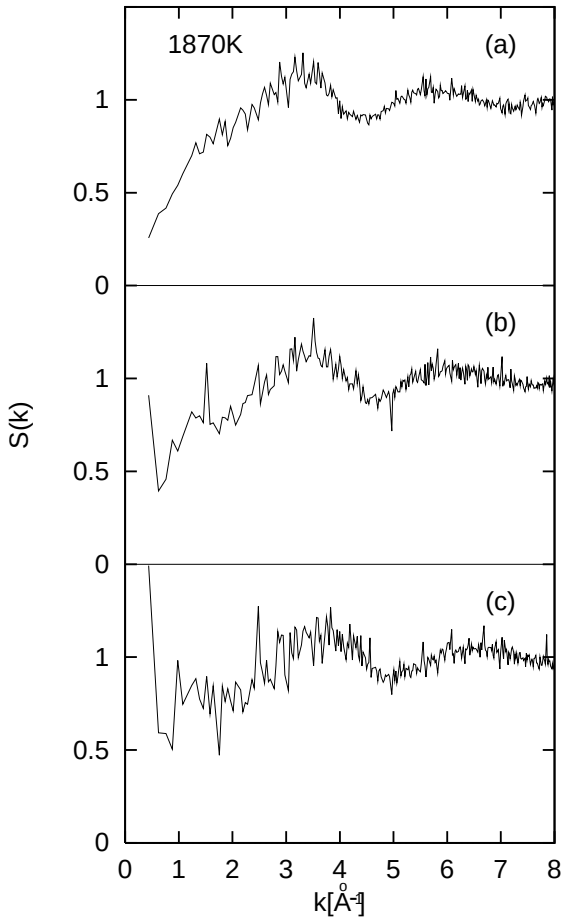

Figure 4. Static structure factors $S(k)$ for calculations at 1870 K and (a) 815 bar, (b) 420 bar, (c) 370 bar.

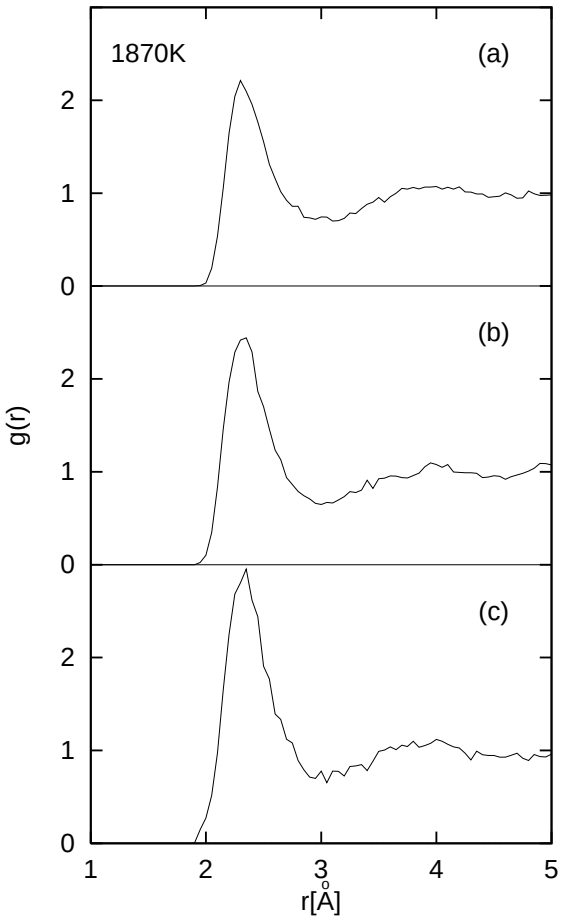

Figure 5. Pair distribution functions $g(r)$ for calculations at 1870 K. The pressures for (a)–(c) are as for figure 4.

critical fluctuations in the static structure factor have been found for expanded liquid mercury by means of FPMD calculations, recently [22]. At the critical point, κ_T should become infinite. However, going to lower wavevectors than in figure 4(c) would require much larger unit cells. The smallest wavevector in our system (0.44 Å^{-1}) is not close enough to zero for a meaningful direct calculation of $\lim_{k\to 0} S(k)$ and κ_T. A comparison of the structure factor at 815 bar (figure 4(a)) with that for the lower temperature at the same pressure (figure 2(b)) shows that they are identical within the range of statistical uncertainty. In contrast to the case for lower pressures, no anomalous behaviour can be found in this case for low wavevectors. For the pair distribution functions in figure 5—even more so than in the case of the lower temperature (figure 3)—no distinct second-neighbour peak can be found. The increase in the height of the first peak going from high pressures (figure 5(a)) to low pressures (figure 5(c)) reflects the scaling of $g(r)$ with the volume per atom in the system. Since the change in density is about 40% going from the highest to the lowest pressure as can be seen from table 1, the effect on the peak height becomes very evident. However, the coordination numbers N_c in table 1 show that the number of first-nearest neighbours even slightly decreases going from high to low pressures. In table 1 self-diffusion coefficients are also given; at 1870 K the values are in

general slightly higher than for 1770 K as would be expected, since the mobility of the atoms increases with temperature. However, there is a local minimum at 420 bar. It is very tempting to assume that this might be related to a critical phenomenon such as long-range ordering. It must be kept in mind, though, that for dynamic properties of a liquid the question of having a large enough number of configurations for time averaging becomes crucial. Additionally, equation (3) is strictly valid only for $t \to \infty$ and our total simulation length of 4.5 ps is rather low.

4. Conclusions

To summarize, we performed FPMD calculations for l-Se at 1770 K at pressures where diffraction experiments have been made previously, and at 1870 K where neither experimental nor theoretical work has been done so far for this system. Our results for the static properties at 1770 K and 815 bar are in very close agreement with the most reliable experimental data which are based on synchrotron radiation. Our calculations at 1870 K correctly predict the expected rise in isothermal compressibility close to the critical point.

Acknowledgments

The work of RS is supported by EPSRC grants GR/L08946 and GR/L38592. Allocations of time on the Cray T3D and T3E at Edinburgh Parallel Computer Centre provided by the UK Car–Parrinello consortium are acknowledged. We would also like to thank D Alfè, F Kirchhoff, M Inui and C Bichara for helpful discussions.

References

[1] Edeling M and Freyland W 1981 *Ber. Bunsenges. Phys. Chem.* **85** 1049
[2] Hoshino H, Schmutzler R W, Warren W W and Hensel F 1976 *Ber. Bunsenges. Phys. Chem.* **80** 27
[3] Tamura K and Hosokawa S 1992 *Ber. Bunsenges. Phys. Chem.* **96** 681
[4] Tamura K 1996 *J. Non-Cryst. Solids* **205–207** 239
[5] Inui M, Noda T and Tamura K 1996 *J. Non-Cryst. Solids* **205–207** 261
[6] Hohl D and Jones R O 1991 *Phys. Rev.* B **43** 3856
[7] Bichara C, Pellegatti A and Gaspard J-P 1994 *Phys. Rev.* B **49** 6581
[8] Raty J Y, Saul A, Gaspard J-P and Bichara C 1999 *Phys. Rev.* B **60** 2441
[9] Kirchhoff F, Gillan M J, Hollender J M, Kresse G and Hafner J 1996 *J. Phys.: Condens. Matter* **8** 9353
[10] Kirchhoff F, Kresse G and Gillan M J 1998 *Phys. Rev.* B **57** 10 482
[11] Wang Y and Perdew J P 1991 *Phys. Rev.* B **44** 13 298
[12] Kresse G, Kirchhoff F and Gillan M J 1999 *Phys. Rev.* B **59** 3501
[13] Shimojo F, Hoshino K, Watabe M and Zempo Y 1998 *J. Phys.: Condens. Matter* **10** 1199
Hoshino K and Shimojo F 1998 *J. Phys.: Condens. Matter* **10** 11 429
[14] Kresse G 1995 *J. Non-Cryst. Solids* **193** 222
[15] Kresse G and Furthmüller J 1996 *Phys. Rev.* B **54** 11 169
[16] Kresse G and Furthmüller J 1996 *Comput. Mater. Sci.* **6** 15
[17] Nosé S 1984 *Mol. Phys.* **52** 255
Hoover W G 1985 *Phys. Rev.* A **31** 1965
[18] Hosokawa S and Tamura K 1990 *J. Non-Cryst. Solids* **117–118** 52
[19] Inui M, Tamura K, Oh'ishi Y, Nakaso I, Funakoshi K and Utsumi W 1999 *J. Non-Cryst. Solids* **250–252** 519
[20] Soldo Y, Hazemann J L, Aberdam D, Inui M, Tamura K, Raoux D and Pernot E 1998 *Phys. Rev.* B **57** 258
[21] Inui M 1998 private communication
[22] Kresse G and Hafner J 1997 *Phys. Rev.* B **55** 7539